Co-ordination Chemistry of Higher Oxidation States. Part 27.[1] Synthesis, Properties, and Electrochemistry of some *cis*-Tetrahalogenoiridium(IV) Complexes: Crystal Structure of [Ir(phen)Cl$_4$]†

Robert A. Cipriano, Lyall R. Hanton, William Levason,* Derek Pletcher, Nigel A. Powell, and Michael Webster
Department of Chemistry, The University, Southampton, SO9 5NH

The iridium(IV) complexes *cis*-[Ir(L–L)Cl$_4$] [L–L = MeSCH$_2$CH$_2$SMe, MeSeCH$_2$CH$_2$SeMe, 2,2′-bipyridyl (bipy), or 1,10-phenanthroline (phen)] have been prepared by Cl$_2$ or HNO$_3$ oxidation of the corresponding Ir^{III} anions [Ir(L–L)Cl$_4$]$^-$. Dark green *cis*-[Ir(L–L)Br$_4$] (L–L = bipy or phen) and *cis*-[Ir(py)$_2$X$_4$] (X = Cl or Br) are also described. Iridium(III) complexes [Ir{RTe(CH$_2$)$_3$TeR}Cl$_4$]$^-$ (R = Me or Ph), [{Ir[Me$_2$Sb(CH$_2$)$_3$SbMe$_2$]Cl$_3$}$_n$], *trans*-[Ir(L–L)$_2$Cl$_2$]$^+$ [L–L = Ph$_2$PCH$_2$CH$_2$PPh$_2$ (dppe), Me$_2$PCH$_2$CH$_2$PMe$_2$ (dmpe), or *o*-C$_6$H$_4$(AsMe$_2$)$_2$], *cis*-[Ir(phen)$_2$Cl$_2$]$^+$, and some rhodium(III) analogues, [Rh(L–L)Cl$_4$]$^-$ (L–L = MeSCH$_2$CH$_2$SMe, MeSeCH$_2$CH$_2$SeMe, or bipy) and *trans*-[Rh(dppe)$_2$Cl$_2$][Rh(dppe)Cl$_4$], are described, but cannot be oxidised to the M^{IV} state. Complexes have been characterised by i.r., u.v.–visible, n.m.r. (^{31}P, ^{77}Se, and ^{125}Te) spectroscopy, and, for the complex [Ir(phen)Cl$_4$], by *X*-ray diffraction. Crystals of [Ir(phen)Cl$_4$] are monoclinic, space group $P2_1/c$ with a = 7.410(8), b = 19.256(4), c = 10.477(4) Å, β = 109.39(6)°, Z = 4, and R = 0.034 for 2 052 reflections. The iridium is six-co-ordinate, Ir–N = 2.042(9), 2.049(9), Ir–Cl = 2.298(3)—2.311(3) Å. The u.v.–visible spectra of the iridium(IV) complexes are interpreted in terms of ligand-to-metal charge-transfer transitions and compared with the analogous *trans*-[IrL$_2$X$_4$]. Electrochemical studies show that for most of the [Ir(L–L)X$_4$]$^-$–[Ir(L–L)X$_4$] couples the electron transfer reaction is close to reversible, with formal potentials for the oxidation occurring at more positive values than for the *trans*-[IrL$_2$X$_4$]$^-$–[IrL$_2$X$_4$] analogues. The rhodium(III) anions show completely irreversible oxidation reactions.

In a previous paper[2] we reported detailed studies of the synthesis, properties, and electrochemistry of a series of iridium(IV) complexes, *trans*-[IrL$_2$X$_4$] [L = pyridine (py), PR$_3$, AsR$_3$, SbR$_3$, SR$_2$, or SeR$_2$; X = Cl or Br]. Only two examples of *cis* isomers, [Ir(py)$_2$Cl$_4$] and [Ir(SbMe$_3$)$_2$Cl$_4$] were obtained in that study. *cis* Stereochemistry can be enforced by the use of chelating bidentate ligands,[3–6] and here we report an investigation of such *cis* isomers with emphasis on the electronic spectral and electrochemical properties.

Experimental

Physical measurements were made as described previously.[2] The following complexes were made by literature methods: *cis*-[Ir(py)$_2$Cl$_4$],[2] *cis*-[Ir(SbMe$_3$)$_2$Cl$_4$],[2] [NMe$_4$][Ir(RSCH$_2$CH$_2$SR)Cl$_4$] (R = Me or Ph),[3] [NMe$_4$][Ir(RSeCH$_2$CH$_2$SeR)Cl$_4$],[4] [NEt$_4$][Ir{MeSe(CH$_2$)$_3$SeMe}Cl$_4$],[4] [NEt$_4$][Ir{MeS(CH$_2$)$_3$SMe}Cl$_4$],[3] [NEt$_4$][Rh(MeSCH$_2$CH$_2$SMe)Cl$_4$],[3] [NMe$_4$][Rh(MeSeCH$_2$CH$_2$SeMe)Cl$_4$],[5] [Hbipy][Rh(bipy)Cl$_4$] (bipy = 2,2′-bipyridine),[7] [NEt$_4$][Ir(MeSCH$_2$CH$_2$SMe)Br$_4$].[3]

trans-*Bis*[1,2-*bis*(*diphenylphosphino*)*ethane*]*dichlororhodium*(III) [1,2-*Bis*(*diphenylphosphino*)*ethane*]*tetrachlororhodate*(III), [Rh(dppe)$_2$Cl$_2$][Rh(dppe)Cl$_4$].—Rhodium(III) chloride hydrate (0.32 g, 1.2 mmol), concentrated hydrochloric acid (2 cm^3), dppe [1,2-bis(diphenylphosphino)ethane] (0.49 g, 1.25 mmol), and [NMe$_4$]Cl (0.15 g, 1.2 mmol) were refluxed together in water–ethanol (2:25 cm^3) for 2.5 h. The cooled mixture was filtered, and the yellow filtrate concentrated to *ca.* 7 cm^3. On standing at 0 °C the yellow solid precipitated (0.39 g, 20%) (Found: C, 57.7; H, 4.6. C$_{78}$H$_{72}$Cl$_6$P$_6$Rh$_2$ requires C, 58.1; H, 4.5%).

trans-*Bis*[1,2-*bis*(*diphenylphosphino*)*ethane*]*dichlororhodium*(III) *Tetrafluoroborate*, [Rh(dppe)$_2$Cl$_2$]BF$_4$.—The above complex was heated in ethanol with dppe [Rh complex : dppe, 1 : 1] for 0.5 h, and excess of 40% HBF$_4$ was added. The pale yellow product precipitated immediately. Yield, quantitative (Found: C, 59.1; H, 4.5. C$_{52}$H$_{48}$BCl$_2$F$_4$P$_4$Rh requires C, 59.1; H, 4.5%).

cis *and* trans *Isomers of Tetrabromobis*(*pyridine*)*iridium*(IV), [Ir(py)$_2$Br$_4$].—Iridium tribromide hydrate (0.47 g, 0.97 mmol) and pyridine (1.0 cm^3, 12.5 mmol) were dissolved in a mixture of water (10 cm^3), ethanol (5 cm^3), and 47% hydrobromic acid (5 cm^3) and the solution was refluxed for 30 min. After cooling, buff crystals of [Hpy][*cis*-Ir(py)$_2$Br$_4$] precipitated and were collected. Excess bromine water was added to the solution causing immediate precipitation of grey-green *trans*-[Ir(py)$_2$Br$_4$][2] which was washed with water and dried *in vacuo* (0.15 g, 23%). [Hpy][*cis*-Ir(py)$_2$Br$_4$] was oxidised by swirling in bromine water, then collecting and drying *in vacuo* the resultant, dark green, *cis*-[Ir(py)$_2$Br$_4$] (0.03 g, 5%) [Found: C, 18.1; H, 1.6; N, 4.1. C$_{10}$H$_{10}$Br$_4$IrN$_2$ (*cis*) requires C, 17.9; H, 1.5; N, 4.2%].

Trichloro(2,6-*ditelluraheptane*)*iridium*(III), [{Ir[MeTe(CH$_2$)$_3$TeMe]Cl$_3$}$_n$].—Iridium trichloride hydrate (0.38 g, 1.1 mmol) and 2,6-ditelluraheptane (0.36 g, 1.1 mmol) were refluxed in ethanol (25 cm^3) for 30 min. After cooling, the brown product was collected on a sinter, washed with ethanol and diethyl ether, and dried *in vacuo* (0.53 g, 78%) (Found: C, 9.5; H, 2.0. C$_5$H$_{12}$Cl$_3$IrTe$_2$ requires C, 9.6; H, 1.9%).

Trichloro[1,3-*bis*(*phenyltelluro*)*propane*]*iridium*(III), [{Ir[PhTe(CH$_2$)$_3$TePh]Cl$_3$}$_n$], was prepared similarly in 76% yield

---

† Tetrachloro(1,10-phenanthroline)iridium(IV).

Supplementary data available: see Instructions for Authors, *J. Chem. Soc., Dalton Trans.*, 1988, Issue 1, pp. xvii—xx.

(Found: C, 23.5; H, 2.3. $C_{15}H_{16}Cl_3IrTe_2$ requires C, 24.0; H, 2.1%).

Tetraethylammonium Tetrachloro(2,6-*ditelluraheptane*)*iridate*(III), $[NEt_4][Ir\{MeTe(CH_2)_3TeMe\}Cl_4]$.—Trichloro(2,6-ditelluraheptane)iridium(III) (0.50 g, 0.8 mmol) and $[NEt_4]Cl\cdot H_2O$ (0.73 g, 4.0 mmol) were refluxed in 2-methoxyethanol (50 cm^3) for 1 h. After cooling, the solution was filtered and the solvent removed *in vacuo*. The resultant oil was treated with ethanol (10 cm^3) and the orange solid thus produced was filtered off, washed with ethanol and diethyl ether, and dried *in vacuo* (0.095 g, 15%) (Found: C, 19.7; H, 3.9; N, 1.6. $C_{13}H_{32}Cl_4IrNTe_2$ requires C, 19.7; H, 4.0; N, 1.8%).

Tetraethylammonium [1,3-*Bis*(*phenyltelluro*)*propane*]*tetrachloroiridate*(III), $[NEt_4][Ir\{PhTe(CH_2)_3TePh\}Cl_4]$, was prepared similarly in 12% yield (Found: C, 30.1; H, 4.2; N, 1.4. $C_{23}H_{36}Cl_4IrNTe_2$ requires C, 30.15; H, 3.9; N, 1.5%).

[1,2-*Bis*(*phenylseleno*)*ethane*]*tribromoiridium*(III), $[\{Ir[PhSe(CH_2)_2SePh]Br_3\}_n]$.—Iridium tribromide hydrate (0.49 g, 1.0 mmol) and 1,2-bis(phenylseleno)ethane (0.34 g, 1.0 mmol) were refluxed in ethanol (20 cm^3) for 2 h. After cooling, the buff product was filtered off, washed with ethanol and diethyl ether, and dried *in vacuo* (0.56 g, 72%) (Found: C, 22.0; H, 1.9. $C_{14}H_{14}Br_3IrSe_2$ requires C, 21.8; H, 1.8%).

Tetraethylammonium [1,2-*Bis*(*phenylseleno*)*ethane*]*tetrabromoiridate*(III), $[NEt_4][Ir\{PhSe(CH_2)_2SePh\}Br_4]$.—[1,2-Bis(phenylseleno)ethane]tribromoiridium(III) (0.50 g, 0.65 mmol) and $[NEt_4]Br\cdot H_2O$ (0.68 g, 3.0 mmol) were refluxed in 2-methoxyethanol (50 cm^3) for 2 h. After cooling, the solution was filtered and the solvent was removed *in vacuo*. The residue was treated with ethanol (10 cm^3) and the resultant fawn solid was filtered off, washed with ethanol and diethyl ether, and dried *in vacuo* (0.24 g, 38%) (Found: C, 27.0; H, 3.6; N, 4.0. $C_{22}H_{34}Br_4IrNSe_2$ requires C, 26.9; H, 3.5; N, 4.0%).

1,10-*Phenanthrolinium Tetrachloro*(1,10-*phenanthroline*)*iridate*(III), $[Hphen][Ir(phen)Cl_4]$.—A solution of 1,10-phenanthroline hydrate (0.61 g, 3.1 mmol) in hot water (40 cm^3) containing concentrated hydrochloric acid (0.04 cm^3) was added to a solution of iridium trichloride hydrate (0.38 g, 1.1 mmol) in a mixture of water (20 cm^3) and hydrochloric acid (5 cm^3). The mixture was boiled for 2 h during which time the orange product precipitated. After cooling the product was filtered off, washed with water, and dried *in vacuo* (0.63 g, 82%) (Found: C, 42.0; H, 2.6; N, 7.9. $C_{24}H_{17}Cl_4IrN_4$ requires C, 41.4; H, 2.4; N, 8.05%).

Tetrachloro(1,10-*phenanthroline*)*iridium*(IV), $[Ir(phen)Cl_4]$.—1,10-Phenanthrolinium tetrachloro(1,10-phenanthroline)iridate(III) (0.1 g, 0.14 mmol) was stirred in concentrated nitric acid (10 cm^3) for 1 min and the mixture was then cooled. The purple-black product was filtered off and dried *in vacuo* (0.057 g, 60%) (Found: C, 27.5; H, 1.7; N, 5.5. $C_{12}H_8Cl_4IrN_2$ requires C, 28.0; H, 1.6; N, 5.4%).

2,2′-*Bipyridinium* (2,2′-*bipyridyl*)*tetrachloroiridate*(III), $[Hbipy][Ir(bipy)Cl_4]$, was prepared similarly to [Hphen][Ir(phen)Cl_4] in 20% yield (Found: C, 36.8; H, 2.4; N, 8.7. $C_{20}H_{17}Cl_4IrN_4$ requires C, 37.1; H, 2.6; N, 8.7%).

(2,2′-*Bipyridyl*)*tetrachloroiridium*(IV), $[Ir(bipy)Cl_4]$.—The salt $[Hbipy][Ir(bipy)Cl_4]$ (0.065 g, 0.1 mmol) was dissolved in a mixture of water (10 cm^3) and concentrated hydrochloric acid (2 cm^3) and the solution was stirred with Dowex 50W cation exchange resin in the H^+ form (20 g) for 10 min. The resin was filtered off and washed with water (200 cm^3). The combined aqueous solutions were reduced to a very small volume and concentrated nitric acid (10 cm^3) was added. After cooling, the purple-black precipitate was filtered off, washed with water, and dried *in vacuo* (0.03 g, 61%) (Found: C, 25.0; H, 1.6; N, 5.6. $C_{10}H_8Cl_4IrN_2$ requires C, 24.5; H, 1.6; N, 5.4%).

1,10-*Phenanthrolinium Tetrabromo*(1,10-*phenanthroline*)*iridate*(III), $[Hphen][Ir(phen)Br_4]$.—A solution of 1,10-phenanthroline hydrate (0.33 g, 1.67 mmol) in hot water (20 cm^3) containing 47% hydrobromic acid (0.1 cm^3) was added to a solution of iridium tribromide hydrate (0.25 g, 0.52 mmol) in water (10 cm^3) and hydrobromic acid (2 cm^3) and the mixture was refluxed for 30 min. After cooling, the red-orange precipitate was filtered off, washed with water and acetone, and dried *in vacuo* (0.32 g, 70%) (Found: C, 33.1; H, 2.0; N, 6.5. $C_{24}H_{17}Br_4IrN_4$ requires C, 33.0; H, 2.0; N, 6.4%).

Tetrabromo(1,10-*phenanthroline*)*iridium*(IV), $[Ir(phen)Br_4]$.—The salt $[Hphen][Ir(phen)Br_4]$ (0.15 g, 0.17 mmol) was stirred in concentrated nitric acid (10 cm^3) for 2 min. The resultant green solid was filtered off, washed with water, and dried *in vacuo* (0.08 g, 68%) (Found: C, 20.9; H, 1.2; N, 4.0. $C_{12}H_8Br_4IrN_2$ requires C, 20.8; H, 1.2; N, 4.0%).

2,2′-*Bipyridinium* (2,2′-*bipyridyl*)*tetrabromoiridate*(III), $[Hbipy][Ir(bipy)Br_4]$, was prepared similarly to [Hphen][Ir(phen)Br_4] (except that refluxing was for 5 h) in 62% yield (Found: C, 29.2; H, 2.2; N, 6.6. $C_{20}H_{17}Br_4IrN_4$ requires C, 29.1; H, 2.1; N, 6.8%).

(2,2′-*Bipyridyl*)*tetrabromoiridium*(IV), $[Ir(bipy)Br_4]$, was prepared from $[Hbipy][Ir(bipy)Br_4]$ in an analogous manner to $[Ir(phen)Br_4]$ in 60% yield (Found: C, 18.0; H, 1.3; N, 4.3. $C_{10}H_8Br_4IrN_2$ requires C, 18.0; H, 1.2; N, 4.2%).

[1,3-*Bis*(*dimethylstibino*)*propane*]*trichloroiridium*(III), $[\{Ir[Me_2Sb(CH_2)_3SbMe_2]Cl_3\}_n]$.—Iridium trichloride hydrate (0.38 g, 1.1 mmol) and 1,3-bis(dimethylstibino)propane (0.38 g, 1.1 mmol) were refluxed in deoxygenated ethanol for 30 min. After cooling the buff precipitate was filtered off, washed with ethanol and diethyl ether, and dried *in vacuo* (0.52 g, 75%) (Found: C, 13.1; H, 2.9. $C_7H_{18}Cl_3IrSb_2$ requires C, 13.0; H, 2.8%).

Trichloro[(o-*phenylenebis*(*diphenylstibine*)]*iridium*(III), $[\{Ir[o\text{-}C_6H_4(SbPh_2)_2]Cl_3\}_n]$, was prepared similarly (3 h reflux) in 59% yield (Found: C, 38.5; H, 2.5. $C_{30}H_{24}Cl_3IrSb_2$ requires C, 38.9; H, 2.6%).

Dichlorobis(1,10-*phenanthroline*)*iridium*(III) *Tetrafluoroborate*, $[Ir(phen)_2Cl_2]BF_4$.—The salt $[Hphen][Ir(phen)Cl_4]$ (0.23 g, 0.33 mmol) was stirred in boiling glycerol (20 cm^3) until the colour changed from orange to dark green. After cooling, excess of a mixture of concentrated hydrochloric acid and 40% tetrafluoroboric acid (1:1, v/v) was added causing precipitation of a yellow-green solid which was filtered off and recrystallised from hot ethanol to give the bright yellow product (0.04 g, 17%) (Found: C, 51.5; H, 1.3; N, 7.8. $C_{24}H_{16}BCl_2F_4IrN_4$ requires C, 51.3; H, 1.1; N, 7.9%).

Bis[1,2-*bis*(*dimethylphosphino*)*ethane*]*dichloroiridium*(III) *Tetrafluoroborate*, $[Ir(dmpe)_2Cl_2]BF_4$.—The iridium(I) complex $[\{IrCl(C_8H_{14})_2\}_2]$ (C_8H_{14} = cyclo-octene) (0.27 g, 0.34 mmol) and 1,2-bis(dimethylphosphino)ethane (dmpe) (0.18 g, 1.2 mmol) were stirred in deoxygenated methanol (30 cm^3) where they quickly reacted to give a yellow solution of $[Ir(dmpe)_2]Cl$. The solution was cooled in ice and chlorine was bubbled through it until the solution became colourless. **CAUTION**. Very exothermic reaction. The solvent was removed *in vacuo* and the residue extracted with boiling water. After cooling, excess of tetrafluoroboric acid–hydrochloric acid was added causing precipitation of the very pale yellow product which was filtered off, washed with water, and dried *in vacuo* (0.16 g, 41%) (Found: C, 22.2; H, 4.8. $C_{12}H_{32}BCl_2F_4IrP_4$ requires C, 22.15; H, 4.9%).

Bis[1,2-*bis*(*diphenylphosphino*)*ethane*]*dichloroiridium*(III) *Tetrafluoroborate*, $[Ir(dppe)_2Cl_2]BF_4$.—The complex $[\{IrCl(C_8H_{14})_2\}_2]$ (0.27 g, 0.34 mmol) and 1,2-bis(diphenylphosphino)ethane (0.51 g, 1.28 mmol) were warmed gently in deoxygenated methanol (30 cm^3) until the colour became red-orange. The solution was then cooled in an ice-bath and chlorine was bubbled through until the colour became pale yellow. On standing in the ice-bath a pale yellow-green precipitate of $[Ir(dppe)_2Cl_2]Cl$ formed and was filtered off and washed with methanol and diethyl ether. This compound was then redissolved in hot ethanol (15 cm^3) and 40% tetrafluoroboric acid was added causing immediate precipitation of the pale yellow-green product (0.28 g, 41%) (Found: C, 54.6; H, 4.4. $C_{52}H_{48}BCl_2F_4IrP_4$ requires C, 54.45; H, 4.2%).

Dichlorobis[o-*phenylenebis*(*dimethylarsine*)]*iridium*(III) *Tetrafluoroborate*, $[Ir(pdma)_2Cl_2]BF_4$.—The complex $[\{IrCl(C_8H_{14})_2\}_2]$ (0.28 g, 0.35 mmol) and *o*-phenylenebis(dimethylarsine) (pdma) (0.36 g, 1.26 mmol) were warmed gently in methanol (30 cm^3) until the solution became orange. The solution was then cooled in an ice-bath and chlorine was bubbled through causing a small amount of $[Ir(pdma)_2Cl_2]Cl$ to precipitate. The solvent was removed *in vacuo* and the crude product was dissolved in boiling water. Excess of 40% tetrafluoroboric acid was added causing immediate precipitation of the pale yellow-green product which was filtered off, washed with water, and dried *in vacuo* (0.29 g, 50%) (Found: C, 26.3; H, 3.7. $C_{20}H_{32}As_4BCl_2F_4Ir$ requires C, 26.0; H, 3.5%).

Crystal-structure Determination.—Dark purple, light-sensitive crystals of $[Ir(phen)Cl_4]$ were obtained by slow cooling over several days from a warm solution of the material dissolved in concentrated nitric acid. Crystals were mounted in thin-walled glass capillaries and preliminary photographic examination established the crystal system and cell dimensions. The crystal density was measured by flotation ($CHCl_3$–$CHBr_3$).

Crystal data. $C_{12}H_8Cl_4IrN_2$, $M = 514.2$, monoclinic, $a = 7.410(8)$, $b = 19.256(4)$, $c = 10.477(4)$ Å, $\beta = 109.39(6)°$, $U = 1\,410.1$ Å^3, $D_m = 2.39(2)$ g cm^{-3}, $Z = 4$, $D_c = 2.421$ g cm^{-3}, $F(000) = 956$, space group $P2_1/c$ (no. 14), λ(Mo-K_α) = 0.710 69 Å, μ(Mo-K_α) = 101.1 cm^{-1}.

Intensity data were recorded on an Enraf-Nonius CAD4 diffractometer equipped with a graphite monochromator and using Mo-K_α radiation. Accurate cell dimensions were obtained from the setting angles of 25 automatically centred reflections and from the same crystal (0.58 × 0.25 × 0.10 mm) at room temperature were recorded 2 759 reflections ($1.5 \leqslant \theta \leqslant 25°$). The check reflections showed no decay during the experiment and a ψ-scan empirical absorption correction was applied to the data (see later). After the data reduction there remained 2 476 unique reflections ($R_{int} = 0.062$) of which 423 [$F < 3\sigma(F)$] were removed leaving 2 053 observed reflections for the analysis and refinement.

Solution and refinement. The normalised structure factors supported the centrosymmetric space group and the direct method strategy (EEES) in SHELX[8] located the Ir, Cl, and N atoms. A structure-factor and electron-density calculation revealed the remaining C atoms. All the non-H atoms were given anisotropic thermal parameters and H-atoms introduced in calculated positions when refinement converged to $R = 0.048$. The difference electron-density synthesis for this model showed several large ($\leqslant 2.61$ e Å^{-3}) peaks about 1.2 Å from the iridium atom which were not chemically significant. The large linear absorption coefficient and the plate-like nature of the crystal suggested that the absorption correction was important and to explore this further, the absorption correction of Walker and Stuart[9] (DIFABS) was applied to the uncorrected data following isotropic refinement. On the basis of the diminution of the spurious peaks in the difference electron density and the reduced R factor, this empirical absorption correction was preferred and subsequent calculations and the final co-ordinates refer to the use of DIFABS.* The 100 reflection appeared to be subject to extinction and was removed from the refinement. Full-matrix least-squares refinement converged to $R = 0.034$ [173 parameters, 2 052 reflections, anisotropic (Ir, Cl, N, C) and isotropic (H) atoms, $w = 1/\sigma^2(F)$, $R' = 0.044$, d(C–H) = 0.95 Å, max. shift/error = 0.23]. A final difference electron-density synthesis showed all features in the range 1.7 to −1.0 e Å^{-3}.

Table 1. Final atomic co-ordinates for $[Ir(phen)Cl_4]$

Atom	*x*	*y*	*z*
Ir	0.548 66(6)	0.357 22(2)	0.175 76(4)
Cl(1)	0.322 4(4)	0.327 3(2)	0.272 9(3)
Cl(2)	0.787 2(5)	0.392 3(2)	0.093 5(3)
Cl(3)	0.310 5(5)	0.389 2(2)	−0.021 4(3)
Cl(4)	0.548 8(5)	0.246 3(1)	0.094 6(3)
N(1)	0.755 6(14)	0.337 5(4)	0.357 1(9)
N(2)	0.567 7(12)	0.452 5(5)	0.266 5(8)
C(1)	0.857 1(17)	0.279 5(5)	0.396 7(13)
C(2)	0.994 0(19)	0.274 7(7)	0.524 9(14)
C(3)	1.026 6(20)	0.327 6(7)	0.617 2(13)
C(4)	0.921 4(14)	0.388 2(6)	0.576 6(11)
C(5)	0.789 1(14)	0.391 6(6)	0.445 4(10)
C(6)	0.688 7(12)	0.453 9(5)	0.396 2(10)
C(7)	0.718 3(15)	0.512 5(5)	0.477 6(11)
C(8)	0.613 6(17)	0.573 3(5)	0.418 1(12)
C(9)	0.507 1(16)	0.571 1(5)	0.288 9(13)
C(10)	0.474 3(16)	0.511 5(6)	0.209 8(13)
C(11)	0.946 6(15)	0.449 6(6)	0.659 3(12)
C(12)	0.846 6(15)	0.509 6(6)	0.610 8(11)

Atomic scattering factors for neutral atoms and anomalous dispersion corrections were taken from SHELX[8] (Cl, N, C, H) and ref. 10 (Ir) and all calculations were performed on an IBM 3090 computer using the programs SHELX,[8] DIFABS,[9] PLUTO,[11] and ORTEP.[12] The final atomic co-ordinates are presented in Table 1.

Additional material available from the Cambridge Crystallographic Data Centre comprises H-atom co-ordinates, thermal parameters, remaining bond lengths and angles, and comparison of bond lengths from the two absorption corrections.

Results and Discussion

The three synthetic routes to *cis*-$[Ir(L–L)X_4]$ (L–L = bidentate ligand) are summarised below, (1)—(3). As found for the complexes with monodentate ligands, the key intermediates are the Ir^{III} anions $[Ir(L–L)X_4]^-$, since bis(ligand) complexes $[Ir(L–L)_2X_2]^+$ are neither oxidised themselves nor easily converted to $[Ir(L–L)X_4]$.

$$IrX_3{\cdot}nH_2O + HX + 2\ L\text{–}L \longrightarrow [H(L\text{–}L)][Ir(L\text{–}L)X_4] \xrightarrow[HNO_3]{X_2\text{ or}} [Ir(L\text{–}L)X_4] \quad (1)$$

(X = Cl or Br, L–L = 2 py, phen, or bipy)

---

* Although the basis of the two empirical absorption corrections is very different, the bond lengths and angles derived from the resulting atomic co-ordinates are in good agreement with the differences <2σ (see Supplementary material).

$$IrX_3\cdot nH_2O + L\text{–}L + [NR_4]X \longrightarrow [NR_4][Ir(L\text{–}L)X_4] \xrightarrow{X_2} [Ir(L\text{–}L)X_4] \quad (2)$$
$$(L\text{–}L = \text{dithioether})$$

$$IrX_3\cdot nH_2O + L\text{–}L \longrightarrow [\{Ir(L\text{–}L)X_3\}_n] \xrightarrow{[NR_4]X} [NR_4][Ir(L\text{–}L)X_4] \xrightarrow{X_2} [Ir(L\text{–}L)X_4] \quad (3)$$
$$(L\text{–}L = \text{diseleno- or ditelluro-ether or distibine})$$

The complex *cis*-$[Ir(py)_2Cl_4]$ is obtained in poor yield by route (1), along with much larger amounts of the *trans* isomer. Trimethylstibine, exceptionally, affords only *cis*-$[Ir(SbMe_3)_2Cl_4]$, but for other monodentate Group 5B ligands only *trans*-$[IrL_2X_4]$ have been isolated.[2] Routes (2) and (3) have been used to prepare $[Ir\{RS(CH_2)_nSR\}Cl_4]$ and $[Ir\{RSe(CH_2)_nSeR\}Cl_4]$ (R = Me or Ph, $n = 2$; R = Me, $n = 3$),[3,4] and new ditelluroether anions $[Ir\{RTe(CH_2)_3TeR\}Cl_4]^-$ (R = Me or Ph) have been obtained by route (3), but decompose with loss of the neutral ligand on attempted oxidation.

Numerous attempts to prepare $[Ir(L\text{–}L)Cl_4]^-$ (L–L = diphosphine or diarsine) by reaction of the ligands with $IrCl_3\cdot nH_2O$ under a wide variety of conditions, and with cations including $[NBu_4]^+$, $[PPh_4]^+$, and $[N(PPh_3)_2]^+$ have been unsuccessful. Examination of the products of the reactions of $IrCl_3\cdot nH_2O$ with $Ph_2PCH_2CH_2PPh_2$ (dppe) in ethanol by ^{31}P n.m.r. spectroscopy, revealed that at least six species were present including *trans*-$[Ir(dppe)_2Cl_2]^+$ and *trans*-$[IrH(dppe)_2Cl]^+$.[13] In contrast tertiary distibines, including $Me_2Sb(CH_2)_3SbMe_2$ and *o*-$C_6H_4(SbPh_2)_2$ react with $IrCl_3\cdot nH_2O$ in ethanol to produce insoluble fawn $[\{Ir(L\text{–}L)Cl_3\}_n]$ complexes, probably halide-bridged polymers; but, unlike the analogues with diseleno- or ditelluro-ethers, conversion to $[Ir(L\text{–}L)Cl_4]^-$ with $[NR_4]Cl$ fails. In Bu^tOH or diglyme [1,1′-oxybis(2-methoxyethane)] $[\{Ir(L\text{–}L)Cl_3\}_n]$ and $[NB^{un}{}_4]Cl$ did not react, whilst in 2-methoxyethanol or *N*,*N*-dimethylformamide (dmf) carbonyl abstraction from the solvent occurred to give fawn materials [ν(CO) *ca.* 2 040 cm^{-1}) {*cf.* $[Ir(CO)(SbR_3)_2Cl_3]$[14]}. The $[\{Ir(L\text{–}L)Cl_3\}_n]$ complexes are not oxidised by $Cl_2\text{–}CCl_4$ or HNO_3, again in contrast to $[\{Ir(SbPh_3)_2Cl_3\}_n]$ which rapidly oxidises to *trans*-$[Ir(SbPh_3)_2Cl_4]$.[2]

cis-Iridium(IV) bromo complexes have not been reported previously. Dark green *cis*-$[Ir(py)_2Br_4]$ is easily obtained by bromine water oxidation of [Hpy][*cis*-$Ir(py)_2Br_4$], itself a minor by-product of the reaction of $IrBr_3\cdot nH_2O$, py, and HBr in aqueous ethanol. Intensely green $[Ir(L\text{–}L)Br_4]$ (L–L = phen or bipy) are produced in good yield by HNO_3 oxidation [route (1)]. Iridium(IV) bromo complexes with Group 6B ligands have not been obtained: $[NR_4][Ir(L\text{–}L)Br_4]$ (L–L = dithio- or diseleno-ether) are readily prepared, but attempted oxidation with Br_2 or HNO_3 failed. Four $[Ir(L\text{–}L)_2Cl_2]^+$ cations, *cis*-$[Ir(phen)_2Cl_2]^+$[6] and *trans*-$[Ir(L\text{–}L)_2Cl_2]^+$ [L–L = $Me_2PCH_2CH_2PMe_2$, *o*-$C_6H_4(AsMe_2)_2$, or $Ph_2PCH_2CH_2PPh_2$] were prepared, but are not chemically oxidised to Ir^{IV}.

In marked contrast to the complex mixture produced with $IrCl_3\cdot nH_2O$, we find that dppe reacts with $RhCl_3\cdot 3H_2O$ in a 1 : 1 mol ratio in ethanol to produce *trans*-$[Rh(dppe)_2Cl_2][Rh(dppe)Cl_4]$, identified by its characteristic ^{31}P n.m.r. spectrum (Table 2). Attempts to isolate $[Rh(dppe)Cl_4]^-$ with other large cations failed, $[Rh(dppe)_2Cl_2][Rh(dppe)Cl_4]$ being produced in every case, but since *trans*-$[Rh(dppe)_2Cl_2]BF_4$ can be isolated using excess dppe, the properties of the rhodium anion can be inferred by comparison of the properties of the two complexes. No chemical oxidation of $[Rh(dppe)Cl_4]^-$ or $[Rh(L\text{–}L)Cl_4]^-$ (L–L = $MeSCH_2CH_2SMe$,[3] $MeSeCH_2CH_2SeMe$,[5] or bipy[7]) by HNO_3 or Cl_2 was observed.

Properties.—The $[Ir(L\text{–}L)Cl_4]$ complexes are deep red-brown or purple, and $[Ir(L\text{–}L)Br_4]$ are dark green solids. All are strong oxidants (see below) and decompose slowly at room temperature. The *trans*-$[IrL_2X_4]$ complexes were very soluble in most common solvents,[2] but *cis*-$[Ir(L\text{–}L)X_4]$ are only slightly soluble in MeCN or CH_2Cl_2, more soluble in Me_2SO (dmso) or dmf, and decomposed or were insoluble in other common solvents. As expected for $t_{2g}{}^5$ Ir^{IV}, the $\mu_{eff.}$ values are in the range of 1.4—1.7.[3,4] Comparison of the far-i.r. spectra of corresponding Ir^{III} and Ir^{IV} complexes allows the assignment of several strong or medium intensity bands in each as ν(Ir–X) modes consistent with *cis*-IrX_4 groups (theory 4, $2A_1 + B_1 + B_2$), oxidation of Ir^{III} to Ir^{IV} producing small (10—20 cm^{-1}) high frequency shifts in all bands. Confirmation of the presence of

Table 2. Selected spectroscopic data for Rh^{III} and Ir^{III} ions

Complex	$\nu(M\text{–}X)/cm^{-1}$	N.m.r. data[a]
[Hpy][*cis*-$Ir(py)_2Cl_4$]	346, 328, 272	
$[Hbipy][Ir(bipy)Cl_4]$	333, 316(sh), 309, 300(sh)	
$[Hbipy][Ir(bipy)Br_4]$	222, 207	
$[Hphen][Ir(phen)Cl_4]$	340, 304, 291	
$[Hphen][Ir(phen)Br_4]$	230, 221	
$[\{Ir[Me_2Sb(CH_2)_3SbMe_2]Cl_3\}_n]$	317, 309(sh), 282	
$[\{Ir[o\text{-}C_6H_4(SbPh_2)_2]Cl_3\}_n]$	321, 275	
$[\{Ir[MeTe(CH_2)_3TeMe]Cl_3\}_n]$	316, 284(sh)	
$[\{Ir[PhTe(CH_2)_3TePh]Cl_3\}_n]$	316, 300(sh), 258	
$[NEt_4][Ir\{MeTe(CH_2)_3TeMe\}Cl_4]$	304, 279	$\delta(^{125}Te) = 362.5, 357.5$[b]
$[NEt_4][Ir\{PhTe(CH_2)_3TePh\}Cl_4]$	305, 279	$\delta(^{125}Te) = 541.1, 532.7$[b]
$[\{Ir(PhSeCH_2CH_2SePh)Br_3\}_n]$	226	
$[NEt_4][Ir(PhSeCH_2CH_2SePh)Br_4]$	214, 200(sh)	$\delta(^{77}Se) = 456.6, 452.3$[c]
trans-$[Ir(Ph_2PCH_2CH_2PPh_2)_2Cl_2]BF_4$	327	$\delta(^{31}P) = +2.6$[d]
trans-$[Ir\{o\text{-}C_6H_4(AsMe_2)_2\}_2Cl_2]BF_4$	337	
trans-$[Ir(Me_2PCH_2CH_2PMe_2)_2Cl_2]BF_4$		$\delta(^{31}P) = +2.7$[d]
cis-$[Ir(phen)_2Cl_2]BF_4$	336, 319	
trans-$[Rh(Ph_2PCH_2CH_2PPh_2)_2Cl_2]BF_4$	360	$\delta(^{31}P) = 37.2\ (^1J = 84\ Hz)$[d]
trans-$[Rh(Ph_2PCH_2CH_2PPh_2)_2Cl_2]$-$[Rh(Ph_2PCH_2CH_2PPh_2)Cl_4]$	358, 338, 332(sh), 317	$\delta(^{31}P) = 37.2\ (^1J = 83\ Hz)$ $52.6\ (^1J = 93\ Hz)$[d]

[a] All n.m.r. chemical shifts quoted using the high frequency +ve convention. [b] Relative to neat external $TeMe_2(\delta = 0)$, complex in MeCN solutio [c] Relative to neat external $SeMe_2(\delta = 0)$, complex in MeCN solution. [d] Relative to 85% H_3PO_4, complex in CH_2Cl_2 solution.

Table 3. Spectroscopic data for iridium(IV) complexes

Complex	ν(Ir–X)/cm^{-1}	$10^{-3}E_{max.}$/cm^{-1} (ε_{mol}/dm^{-3} mol^{-1} cm^{-1})*	Solvent
cis-$[Ir(py)_2Cl_4]$	346, 328, 272	15.8(sh), 17.9(sh), 19.1, 20.2(sh), 22.0(sh), 26.1, 30.3	MeCN
cis-$[Ir(py)_2Br_4]$	235, 211	~11.0, 12.75, 14.8, 15.9(sh), 23.1(sh), 27.6(sh)	MeCN
cis-$[Ir(SbMe_3)_2Cl_4]$	355, 341, 314	10.8, 17.6(sh), 20.2, 22.2, 29.4, 32.8(sh)	CH_2Cl_2
$[Ir(bipy)Cl_4]$	344, 336, 320, 314(sh)	16.0, 19.3, 23.0(sh), 26.9(sh)	CH_2Cl_2
$[Ir(phen)Cl_4]$	365, 338, 330(sh), 318(sh)	4.25, 16.4(sh), 19.2, 25.1, 28.6	CH_2Cl_2
$[Ir(bipy)Br_4]$	247(sh), 242, 224, 200	14.3, 14.7, 15.9(sh), 20.8(sh), 24.7	CH_2Cl_2
$[Ir(phen)Br_4]$	248(sh), 239, 203	4.25, 11.1, 14.35, 18.2(sh), 25.0(sh), 27.7(sh), 34.2	CH_2Cl_2
$[Ir(MeSCH_2CH_2SMe)Cl_4]$	336(sh), 328, 316, 303	17.4(450), 19.6(4 675), 22.3(4 940), 26.6(sh), 33.0(1 000)	dmso
$[Ir\{MeS(CH_2)_3SMe\}Cl_4]$	335(sh), 325, 315, 303	16.9(340), 19.65(3 290), 22.4(3 990), 26.7(sh), 34.4(1 296)	dmso
$[Ir(PhSCH_2CH_2SPh)Cl_4]$	336(sh), 329, 318, 305	17.0(300), 19.9(2 950), 22.4(3 500), 28.6(sh), 33.0(1 075)	dmso
$[Ir(MeSeCH_2CH_2SeMe)Cl_4]$	318(sh), 311, 281	17.2(290), 20.0(2 220), 23.4(2 390), 28.6(1 020), 33.0(sh)	dmso
$[Ir\{MeSe(CH_2)_3SeMe\}Cl_4]$	316(br), 298 (sh)	17.2(280), 20.0(2 200), 22.7(2 300), 28.6(1 000)	dmso
$[Ir(PhSeCH_2CH_2SePh)Cl_4]$	316, 313, 302(sh)	17.3(280), 20.0(2 000), 22.7(2 110), 28.3(1 300)	dmso

* In solvent specified. The complexes of the N-donor ligands were poorly soluble and hence reliable ε_{mol} values were not obtained. The solid state (diffuse reflectance) spectra diluted with $BaSO_4$ were very similar in profile and energy to the solution spectra.

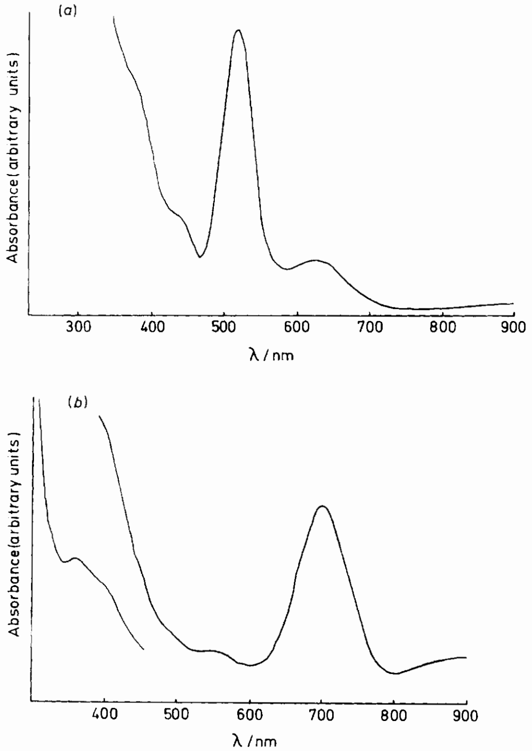

Figure 1. (*a*) U.v.–visible spectrum of $[Ir(bipy)Cl_4]$ in MeCN, (*b*) u.v.–visible spectrum of $[Ir(phen)Br_4]$ in MeCN

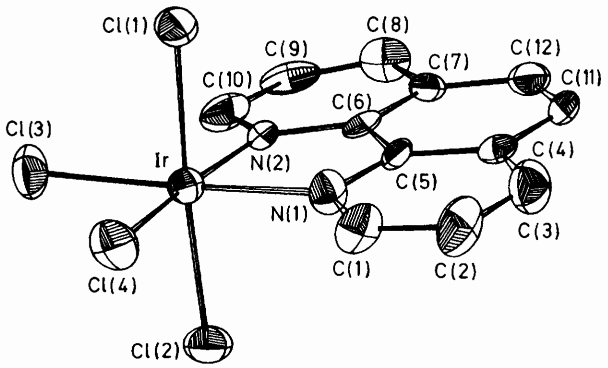

Figure 2. Discrete molecule of $[Ir(phen)Cl_4]$ showing the atom numbering scheme. The thermal ellipsoids are drawn with a 50% probability surface and H-atoms are omitted for clarity

chelated L–L comes from the n.m.r. spectra (^1H,[15] $^{77}Se\{^1H\}$, or $^{125}Te\{^1H\}$ as appropriate), of the Group 6B donor ligand complexes $[Ir(L-L)X_4]^-$, which are characteristic of the presence of two diastereoisomers of the chelated ligand resulting from slow pyramidal inversion; and for $[Ir(phen)Cl_4]$ by an *X*-ray study (see later).

The $[Ir(L-L)X_4]$ complexes have characteristic u.v.–visible spectra (see Table 3), and typical examples are shown in Figure 1. From previous studies of $[IrX_6]^{2-}$ (ref. 16) and *trans*-$[IrL_2X_4]$,[2] with the exception of weak features $\leqslant$5 000 cm^{-1}, which are intraconfigurational in origin, the spectra are expected to consist of ligand-to-metal charge-transfer (l.m.c.t.) transitions. For the high symmetry (D_{4h}) *trans*-$[IrL_2X_4]$ assignments of the spectra in terms of discrete $\pi_X, \sigma_X, \sigma_L \longrightarrow Ir(t_{2g})$ l.m.c.t. transitions proved possible, but the lower symmetry (C_{2v}) of the compound *cis*-$[Ir(L-L)X_4]$ results in significant mixing of Ir–L and Ir–X orbitals, making assignments of bands as either X → Ir *or* L → Ir less justified. A further result of this orbital mixing is that the spectra show less pronounced changes with variation of L–L (constant X) (Table 3). Nonetheless, comparison of the spectra of $[Ir(L-L)Cl_4]$ with those of the *trans*-$[IrL_2Cl_4]$ with the same donor set, or, where available, with $[Ir(L-L)Br_4]$, allows some tentative assignments. Thus the band or bands at *ca.* 17 000—23 000 cm^{-1} in the chlorides have substantial $\pi_{Cl} \longrightarrow Ir$ (t_{2g}) l.m.c.t. character, whilst the $\sigma_{Cl} \longrightarrow Ir$ (t_{2g}) transitions are at *ca.* 28 000 cm^{-1}. For the S or Se ligand complexes no bands assignable to transitions from the Group 6B element were observed, but for the N-donor heterocycle complexes a weak band at *ca.* 16 000 cm^{-1} may be $\pi_L \longrightarrow Ir$ l.m.c.t. The spectra of the 2,2′-bipyridyl and 1,10-phenanthroline complexes are complicated above 25 000 cm^{-1} and are not readily assigned. Similar problems have been encountered in the isoelectronic Ru^{III} and Os^{III} analogues.[17] For the bromo complexes, $\pi_{Br} \longrightarrow Ir$ (t_{2g}) l.m.c.t. bands are found at 12 000—15 000 cm^{-1}.

Structure of $[Ir(phen)Cl_4]$.—The structure consists of discrete molecules, shown in Figure 2, with the expected octahedral co-ordination of the Ir atom. The molecule has no crystallographic symmetry but inspection of the bond lengths and angles, Table 4, shows approximate C_s symmetry [the mirror plane passing through Cl(1) and Cl(2)] rather than C_{2v}. The compounds most closely related appear to be *trans*-$[Ir(PR_3)_2Cl_4]$[18] containing Ir^{IV} and the Ir^{III} chloro species *trans*-[Ir(SMe$_2$)$_2$Cl$_4$]$^-$[19] and *trans*-[Ir(py)$_4$Cl$_2$]$^+$.[20] Comparison of the Ir–Cl distances in these and the present compound shows Ir^{IV}–Cl distances are shorter by *ca.* 0.05 Å than the Ir^{III}–Cl ones and that within the four Ir–Cl distances in [Ir(phen)Cl$_4$] there is no recognisable systematic variation with position relative to the nitrogen atoms ('*trans* influence'). The 1,10-phenanthroline ligand has been characterised on many occasions[21,22] and this further example shows planar rings (maximum deviation 0.03 Å) with a small dihedral angle between adjacent rings (3.8, 3.1°) giving the ligand a slight curvature.[21,23] Bond distances in the N-ligand are unexceptional but the structure provides the first example of an octahedral Ir^{IV} [Ir(L–L)Cl$_4$]-type complex.

Electrochemistry.—Cyclic voltammetry (at four potential scan rates, 0.05—0.30 V s^{-1}) at a vitreous carbon disc electrode was used to investigate the electrochemistry of 14 iridium couples, [Ir(L–L)X$_4$]$^-$–[Ir(L–L)X$_4$]. Experiments were carried out with solutions approximately 1 mmol dm^{-3} in an iridium complex and containing [NBu^n$_4$]BF$_4$ (0.2 mol dm^{-3}). The solvent of choice was MeCN but low solubility also led to CH$_2$Cl$_2$ and dmf being used; the Ir^{IV} complexes were particularly difficult to dissolve and hence most cyclic voltammograms were obtained for solutions of the iridium(III) complexes.

Figure 3 shows the set of cyclic voltammograms (c.v.) recorded for [Ir(PhSCH$_2$CH$_2$SPh)Cl$_4$]$^-$ in MeCN. It can be seen that the responses have the characteristic shapes for a reversible one-electron oxidation process, and this conclusion is confirmed by quantitative analysis of the curves.[24–26] Hence it is concluded that the couple [Ir(PhSCH$_2$CH$_2$SPh)Cl$_4$]$^-$–[Ir(PhSCH$_2$CH$_2$SPh)Cl$_4$] is rapid, with a formal potential of 1.21 V *versus* s.c.e. (saturated calomel electrode) and that the Ir^{IV} complex is stable, at least on the time-scale of a few minutes. No further oxidation or reduction processes were observed when the potential limits were extended. This simple electrochemistry is typical of all the couples [Ir(L–L)X$_4$]$^-$–[Ir(L–L)X$_4$] investigated, except for those with L–L = RTe(CH$_2$)$_3$TeR where the cyclic voltammograms of the Ir^{III} anions show only an irreversible oxidation process. The Ir^{IV} complexes are not stable when the donor atoms are tellurium, as was previously observed with Me$_2$Te.[2]

Table 5 reports the formal potentials for the couples which show reversible electron transfer, both in the solvent used for the experiment and converted to an acetonitrile scale; this conversion has been made assuming that the formal potential of the [Fe(η^5-C$_5$H$_5$)$_2$]–[Fe(η^5-C$_5$H$_5$)$_2$]$^+$ couple may be used to correct for liquid junction effects. For the purposes of comparison, the formal potentials of the two *cis* monodentate

Table 4. Selected bond distances (Å) and angles (°) for [Ir(phen)Cl$_4$]

Ir–Cl(1)	2.305(3)	Ir–N(1)	2.042(9)
Ir–Cl(2)	2.310(3)	Ir–N(2)	2.049(9)
Ir–Cl(3)	2.311(3)	Cl ··· Cl(minimum intra)	3.28
Ir–Cl(4)	2.298(3)	N(1) ··· N(2)(intra)	2.62
N(1)–C(1)	1.33(1)	C(5)–C(6)	1.42(1)
N(1)–C(5)	1.36(1)	C(6)–C(7)	1.39(1)
N(2)–C(6)	1.36(1)	C(7)–C(8)	1.43(2)
N(2)–C(10)	1.36(1)	C(8)–C(9)	1.32(2)
C(1)–C(2)	1.39(2)	C(9)–C(10)	1.39(2)
C(2)–C(3)	1.37(2)	C(4)–C(11)	1.44(2)
C(3)–C(4)	1.39(2)	C(11)–C(12)	1.38(2)
C(4)–C(5)	1.40(1)	C(12)–C(7)	1.40(2)
Cl(1)–Ir–Cl(2)	175.5(1)	N(1)–Ir–Cl(1)	88.5(3)
Cl(1)–Ir–Cl(3)	90.6(1)	N(1)–Ir–Cl(2)	88.3(3)
Cl(1)–Ir–Cl(4)	91.2(1)	N(1)–Ir–Cl(3)	174.8(3)
Cl(2)–Ir–Cl(3)	92.3(1)	N(1)–Ir–Cl(4)	94.5(3)
Cl(2)–Ir–Cl(4)	92.3(1)	N(2)–Ir–Cl(1)	88.1(3)
Cl(3)–Ir–Cl(4)	90.6(1)	N(2)–Ir–Cl(2)	88.1(3)
N(1)–Ir–N(2)	79.6(3)	N(2)–Ir–Cl(3)	95.2(2)
		N(2)–Ir–Cl(4)	174.1(2)

Internal ring of C$_{12}$H$_8$N$_2$ (phen) (N–C–C, C–N–C, C–C–C)
Minimum: 116(1) Maximum: 124(1)

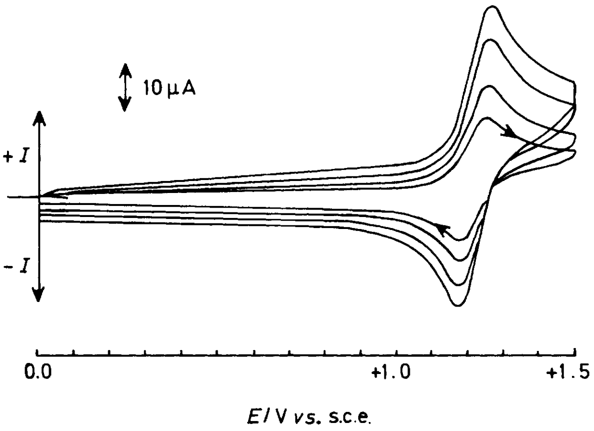

Figure 3. Cyclic voltammogram of [NMe$_4$][Ir(PhSCH$_2$CH$_2$SPh)Cl$_4$] at potential scan rates of 0.05, 0.1, 0.2, and 0.3 V s^{-1}

Table 5. Cyclic voltammetric data for the iridium complexes

Couple	Solvent	$E^{\ominus}_{e}$/V *vs.* s.c.e.*
cis-[Ir(py)$_2$Cl$_4$]–*cis*-[Ir(py)$_2$Cl$_4$]$^-$	MeCN	1.08
cis-[Ir(py)$_2$Br$_4$]–*cis*-[Ir(py)$_2$Br$_4$]$^-$	dmf	0.88(0.88)
[Ir(phen)Cl$_4$]–[Ir(phen)Cl$_4$]$^-$	MeCN	1.10
[Ir(phen)Br$_4$]–[Ir(phen)Br$_4$]$^-$	dmf	1.07(1.07)
[Ir(bipy)Cl$_4$]–[Ir(bipy)Cl$_4$]$^-$	MeCN	1.05
[Ir(bipy)Br$_4$]–[Ir(bipy)Br$_4$]$^-$	CH$_2$Cl$_2$	1.16(1.10)
[Ir(MeSCH$_2$CH$_2$SMe)Cl$_4$]–[Ir(MeSCH$_2$CH$_2$SMe)Cl$_4$]$^-$	MeCN	1.20
[Ir(MeSCH$_2$CH$_2$SMe)Br$_4$]–[Ir(MeSCH$_2$CH$_2$SMe)Br$_4$]$^-$	dmf	1.19(1.19)
[Ir(PhSCH$_2$CH$_2$SPh)Cl$_4$]–[Ir(PhSCH$_2$CH$_2$SPh)Cl$_4$]$^-$	MeCN	1.21
[Ir(MeSCH$_2$CH$_2$CH$_2$SMe)Cl$_4$]–[Ir(MeSCH$_2$CH$_2$CH$_2$SMe)Cl$_4$]$^-$	MeCN	1.12
[Ir(MeSeCH$_2$CH$_2$SeMe)Cl$_4$]–[Ir(MeSeCH$_2$CH$_2$SeMe)Cl$_4$]$^-$	MeCN	1.12
[Ir(PhSeCH$_2$CH$_2$SePh)Cl$_4$]–[Ir(PhSeCH$_2$CH$_2$SePh)Cl$_4$]$^-$	MeCN	1.14
[Ir(PhSeCH$_2$CH$_2$SePh)Br$_4$]–[Ir(PhSeCH$_2$CH$_2$SePh)Br$_4$]$^-$	CH$_2$Cl$_2$	1.22(1.16)
[Ir(MeSeCH$_2$CH$_2$CH$_2$SeMe)Cl$_4$]–[Ir(MeSeCH$_2$CH$_2$CH$_2$SeMe)Cl$_4$]$^-$	MeCN	1.05
[Fe(η^5-C$_5$H$_5$)$_2$]$^+$–[Fe(η^5-C$_5$H$_5$)$_2$]	MeCN	0.40

* $E^{\ominus}_{e}$(MeCN)/V *vs.* s.c.e. are shown in parentheses.

Table 6. Oxidation potentials for some Rh^{III} anions

Complex	E_p^{ox}/V *vs.* s.c.e.[a]
$[Rh(py)_2Cl_4]^-$	1.22
$[Rh(bipy)Cl_4]^-$	1.38
$[Rh(PEt_3)_2Cl_4]^-$	1.26
$[Rh(Ph_2PCH_2CH_2PPh_2)Cl_4]^-$	1.89
$[Rh(SMe_2)_2Cl_4]^-$	1.64
$[Rh(MeSCH_2CH_2SMe)Cl_4]^-$	1.78[b]
$[Rh(SeMe_2)_2Cl_4]^-$	1.55
$[Rh(MeSeCH_2CH_2SeMe)Cl_4]^-$	1.62

[a] Oxidation potentials for Rh^{III} anions in MeCN–$[NBu^n_4]BF_4$ (0.1 mol dm^{-3}), measured by cyclic voltammetry at 0.1 V s^{-1} at a vitreous carbon electrode. [b] Solvent is CH_2Cl_2.

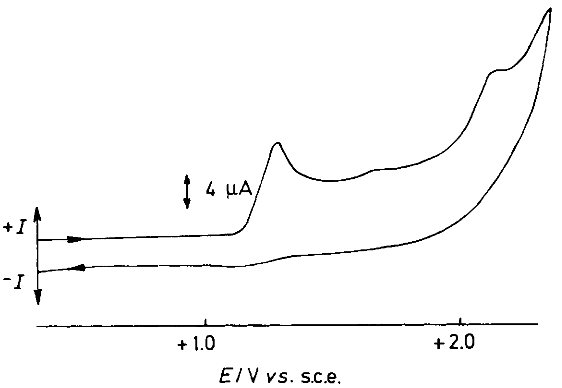

Figure 4. Cyclic voltammogram for $[PEt_3H][Rh(PEt_3)_2Cl_4]$ at a potential scan rate of 0.3 V s^{-1}

ligand complexes are also included. It should be noted that formal potentials of the bidentate ligand complex couples are less sensitive to ligand than is the case for the *trans*-$[IrL_2X_4]^-$–$[IrL_2X_4]$ couples.[2] This mirrors the influence of the structure upon the u.v.–visible spectra. For S and Se donor ligands, the potentials of the chloro and bromo derivatives are very similar, and it is interesting to note that the bidentate ligands giving six-membered rings stabilise Ir^{IV} more successfully than ligands giving smaller rings.

Cyclic voltammograms were also recorded in MeCN for the complexes $[Ir(L–L)_2Cl_2]^+$, with L–L = phen, dppe, *o*-phenylenebis(dimethylarsine), or 1,2-bis(dimethylphosphino)ethane, but these Ir^{III} complexes did not show any oxidation processes even when the potential limit was extended to +2.4 V. Warren and Bennett[27] also report the absence of either chemical or electrochemical oxidation in such complexes and the stability to oxidation of the t_{2g}^6 Ir^{III} in these complexes compared to $[Ir(L–L)X_4]$ or $[IrL_2X_4]$ types is due to the much greater ligand field stabilisation energy. In contrast, the $[Ir(L–L)_2Cl_2]^+$ complexes can be reduced electrochemically but the cyclic voltammograms are complex since the reduced species lose Cl^- with rates which depend strongly upon the medium. Several papers have discussed the mechanism of these reductions,[28–32] and it will also be the subject of further investigations.

The oxidation of the Rh^{III} complexes of types $[RhL_2Cl_4]^-$ and $[Rh(L–L)Cl_4]^-$ was investigated by cyclic voltammetry. The oxidation occurs only at rather positive potentials and several anodic peaks are commonly observed. In all cases the first oxidation process is observed as a well formed, although totally irreversible, anodic peak on the voltammogram. A typical curve is shown in Figure 4. A comparison of the peak current densities with that for ferrocene would suggest the oxidation involves a single electron. Thus it appears that the Rh^{III}–Rh^{IV} couples may be observed but the Rh^{IV} complexes are not stable even on the time-scale of cyclic voltammetry. The oxidation potentials for the eight Rh^{III} complexes are reported in Table 6. Although, because the electrode reactions are irreversible, it is not possible to determine formal potentials for the Rh^{III}–Rh^{IV} couples, it is interesting to note that there is a linear correlation between the oxidation potentials of the Rh^{III} anions and the formal potentials of the corresponding Ir^{III}–Ir^{IV} couples (Figure 5). This indicates that the same factors determine the oxidation potentials for the complexes of the two metals.

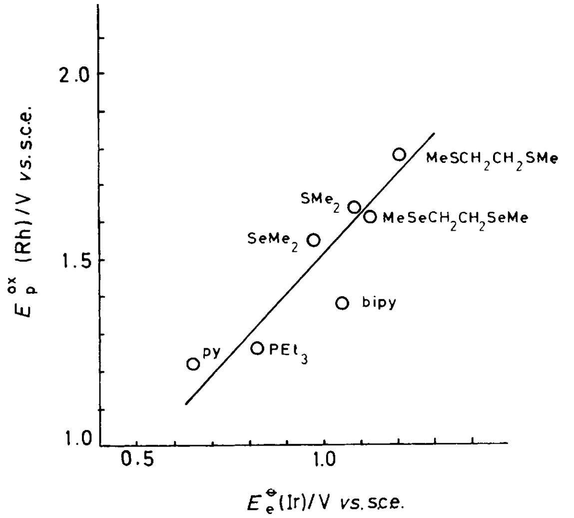

Figure 5. The relationship between $E_e^{\ominus}$ for the Ir complexes and E_p^{ox} for the analogous Rh complexes

Acknowledgements

We thank the S.E.R.C. for support and for a postgraduate studentship (to N. A. P.), and Dr. M. B. Hursthouse for the *X*-ray data collection on the S.E.R.C.–Q.M.C. diffractometer. We also thank the Dow Chemical Company, U.S.A., for leave of absence granted for postgraduate studies (to R. A. C.).

References

1 Part 26, W. Levason, M. D. Spicer, and M. Webster, *J. Chem. Soc., Dalton Trans.*, 1988, 1377.
2 R. A. Cipriano, W. Levason, D. Pletcher, N. A. Powell, and M. Webster, *J. Chem. Soc., Dalton Trans.*, 1987, 1901.
3 D. J. Gulliver, W. Levason, K. G. Smith, M. J. Selwood, and S. G. Murray, *J. Chem. Soc., Dalton Trans.*, 1980, 1718.
4 E. G. Hope, W. Levason, M. Webster, and S. G. Murray, *J. Chem. Soc., Dalton Trans.*, 1986, 1003.
5 D. J. Gulliver, E. G. Hope, W. Levason, S. G. Murray, and G. L. Marshall, *J. Chem. Soc., Dalton Trans.*, 1985, 1265.
6 J. A. Bromhead and W. Grumley, *Inorg. Chem.*, 1971, **10**, 2002.
7 E. D. McKenzie and R. A. Plowman, *J. Inorg. Nucl. Chem.*, 1970, **32**, 199.
8 G. M. Sheldrick, SHELX program for crystal structure determination, University of Cambridge, 1976.
9 N. Walker and D. Stuart, DIFABS empirical absorption correction program, University of London, 1982; *Acta. Crystallogr., Sect. A*, 1983, **39**, 158.
10 'International Tables for *X*-Ray Crystallography,' Kynoch Press, Birmingham, 1976, vol. 4, pp. 99–101 and 149–150.
11 W. D. S. Motherwell and W. Clegg, PLUTO program for plotting molecular and crystal structures, Universities of Cambridge and Goettingen, 1978.

12 C. K. Johnson, ORTEP, A Fortran thermal ellipsoid plot program for crystal structure illustrations, Technical Report ORNL-3794, Oak Ridge National Laboratory, Tennessee, 1965.
13 J. S. Miller and K. G. Caulton, *J. Am. Chem. Soc.*, 1975, **97**, 1067.
14 J. Chatt, N. P. Johnson, and B. L. Shaw, *J. Chem. Soc.*, 1964, 1625.
15 D. J. Gulliver, A. L. Hale, W. Levason, and S. G. Murray, *Inorg. Chim. Acta*, 1983, **69**, 25.
16 A. B. P. Lever, 'Inorganic Electronic Spectroscopy,' 2nd edn., Elsevier, Amsterdam, 1984.
17 G. M. Bryant and J. E. Fergusson, *Aust. J. Chem.*, 1971, **24**, 275.
18 L. Aslanov, R. Mason, A. G. Wheeler, and P. O. Whimp, *Chem. Commun.*, 1970, 30.
19 L. R. Gray, D. J. Gulliver, W. Levason, and M. Webster, *Acta Crystallogr., Sect. B*, 1982, **38**, 3079.
20 R. D. Gillard, S. H. Mitchell, P. A. Williams, and R. S. Vagg, *J. Coord. Chem.*, 1984, **13**, 325.
21 B. A. Frenz and J. A. Ibers, *Inorg. Chem.*, 1972, **11**, 1109.
22 P. C. Healy, L. M. Engelhardt, V. A. Patrick, and A. H. White, *J. Chem. Soc., Dalton Trans.*, 1985, 2541.
23 G. Marangoni, B. Pitteri, V. Bertolasi, G. Gilli, and V. Ferretti, *J. Chem. Soc., Dalton Trans.*, 1986, 1941.
24 R. Greef, R. Peat, L. M. Peter, D. Pletcher, and J. Robinson, 'Instrumental Methods in Electrochemistry,' Ellis Horwood, Chichester, 1985.
25 A. J. Bard and L. R. Faulkner, 'Electrochemical Methods,' Wiley, New York, 1980.
26 P. T. Kissinger and W. R. Heineman (eds.), 'Laboratory Techniques in Electroanalytical Chemistry,' Marcel Dekker, New York, 1984.
27 L. F. Warren and M. A. Bennett, *Inorg. Chem.*, 1976, **15**, 3126.
28 S. Roffia and M. Ciano, *J. Electroanal. Chem.*, 1978, **87**, 267.
29 L. J. Kahl, K. W. Hanck, and M. K. DeArmond, *J. Phys. Chem.*, 1978, **82**, 540.
30 B. Divisia-Blohorn, *Inorg. Chim. Acta*, 1986, **117**, 97.
31 B. K. Teo, A. P. Ginsberg, and J. C. Calabrese, *J. Am. Chem. Soc.*, 1976, **98**, 3027.
32 G. Pilloni, G. Zotti, and M. Martelli, *Inorg. Chem.*, 1982, **21**, 1283.

Received 11*th November* 1987; *Paper* 7/2003